Arch. Metall. Mater. **63** (2018), 1, 337-345

DOI: 10.24425/118946

J.J. JASIŃSKI*#, T. FRĄCZEK**, Ł. KURPASKA***, M. LUBAS**, M. SITARZ****

EFFECTS OF DIFFERENT NITRIDING METHODS ON NITRIDED LAYER STRUCTURE AND MORPHOLOGY

The paper presents a comparison of the nitrided layer structure and morphology formed with a conventional controlled gas method, widely use in industrial applications and a layer formed with cathode plasma nitriding (CPN) and active screen plasma nitriding (ASPN). Nitriding processes were realized at 793K for different times and altering parameters, depending on the nitriding process technique. Research have been realized on the Fe Armco material using light microscopy (LM), scanning electron microscopy (SEM, SEM/EBSD), X-ray diffraction (XRD-GID) and atomic force microscopy (AFM). Analysis of the results has confirmed that the structure of the nitrided layer depends mainly on process methodology. In addition Authors has also analyzed kinetics of the process which varies and depends mainly from the surface layer saturation mechanism and nitriding parameters. Acquired knowledge on the structural components of the nitrided layer made it possible to optimize the nitriding parameters in order to reduce or even eliminate the usually unfavorable, brittle compounds and porous zones and of the nitrided layer in the aspect of exploitation properties improvement of the metallic materials.

Keywords: Active Screen Plasma Nitriding (ASPN); nitrided layer; Armco iron; nitriding kinetics, surface morphology

1. Introduction

In the past years of a spectacular development, the surface engineering has taken over modification of the processes used in the industry i.e.: chemical heat treatment – gas nitrding, plasma nitriding. Conventional gas nitriding usually is performed in the temperature range between 753÷853 K, depending on the desired exploitation properties of the nitrided layer. At a lower temperature, processes are realized to obtain structures with improved tribological properties. On the other hand, the higher temperature range is used mostly for the processes which result with the improvement of the corrosion resistance (these processes are widely used for low-carbon and low-alloy steels) [1,2]. The layer obtained after nitriding depends mainly on the temperature, time, atmosphere (the concentration of ammonia, nitrogen) and the chemical composition of the substrate. Typical nitrided layer in steels are analyzed according to phases present in ferrous alloys, and stay in accordance with the Fe-N-C phase diagram. Additionally important and useful in predicting the atmosphere and the nitrided layer composition in gas nitriding processes is Lehrer's diagram. In gas nitriding, to obtain in statu nascendi nitrogen ammonia which dissociates into atomic nitrogen and hydrogen is used. However, nitrogen remains in this state for approx. 1 second and then is combined in a molecule. Thus, in order to provide nitrogen atoms, a continuous flow of ammonia should be applied, including the dissociated ammonia and nitrogen. The thermodynamic activity of nitrogen is determined mainly on the ratio of un-dissociated ammonia partial pressure to hydrogen partial pressure, called the nitriding potential (K_N). Therefore, in order to correct realization of the nitriding process, it is meant to increase the ammonia dissociation rate to the nitrogen sorption, which finally should be faster than diffusion in the substrate [3-5].

During nitriding, the initial effect at the plasma-metal interface is nitrogen chemisorption with the formation of ε-Fe_2N nitride in the surface, called white layer, from which nitrogen diffuses into the substrate. Below this layer, as a result of thermal diffusion, a compound layer $\varepsilon + \gamma'$ is formed which constitutes the solution zone of nitrogen supersaturated ferrite and Fe_4N nitrides precipitations. The stoichiometric morphology of the nitrided layer and phase concentration are functions both of nitrogen concentration, its reactivity with the substrate and temperature [6]. Nitrogen diffusion towards substrate starts mainly from the chemical potential gradient on the gas phase – substrate interface and is a reactive diffusion where Fe_xN_y compounds are formed and change their chemical composition accordingly to nitrogen concentration increment in the substrate. While ferrite [Fe_α(N,C)] is being saturated with nitrogen to the concentration limit, the γ'-Fe_4N phase is formed with shape of brittle coarse needles which are unfavorable with the mechanical properties of nitride layer.

* CZESTOCHOWA UNIVERSITY OF TECHNOLOGY, LOGISTICS AND INTERNATIONAL MANAGEMENT INSTITUTE, AV. ARMII KRAJOWEJ 19B, 42-200 CZESTOCHOWA, POLAND
** CZESTOCHOWA UNIVERSITY OF TECHNOLOGY, MATERIALS SCIENCE INSTITUTE, AV. ARMII KRAJOWEJ 19A, 42-200 CZESTOCHOWA, POLAND
*** NATIONAL CENTRE FOR NUCLEAR RESEARCH, ST. A. SOLTANA 7/23, OTWOCK-SWIERK, POLAND
**** AGH UNIVERSITY OF SCIENCE AND TECHNOLOGY CRACOW, DEPARTMENT OF MATERIALS SCIENCE AND CERAMICS, AL.MICKIEWICZA 30, 30-059 KRAKÓW
# Corresponding author: jarjasinski@o2.pl

Controlled gas nitriding, due to numerous advantages, is currently the most commonly used nitriding technology. Among the most significant advantages of gas nitriding process one can name: (i) generating nitrided layers of a desired phase structure due to adjusting and controlling the nitrogen potential, (ii) controlling of the nitrogen concentration in the ε-$Fe_{2-3}N$ phase to avoid zone porosity and brittleness, (iii) the ability to generate low-temperature nitrogen-related processes, such as: oxy-nitriding, sulfo-nitriding, oxy-carbo-nitriding processes, (iv) the ability to automate processes and technological lines for the process, in order to achieve their high repeatability. However, due to the possibility of limiting ammonia consumption and process effectiveness improvement, gas nitriding processes are increasingly being replaced with plasma nitriding technologies also implemented in a wide range of industries [7]. This is also associated to the numerous advantages of plasma nitriding methods. One of the most significant are: energy saving (even up to about 50% compared to conventional controlled gas nitriding) and the related low consumption of gas media to generate nitriding atmosphere; the ability to formation of the structure of nitrided layers with stress states and properties according to their implementation and finally the repeatability of the process results [8]. In addition, an important aspect of plasma nitriding is the physical surface activation process directly in the reactive chamber as a result of ion bombardment and sputtering effect. Due to this advantage it is possible to realize nitriding process of materials such as stainless steels, light alloys, etc. Intensification of diffusion effects in the plasma nitriding in compare to controlled gas nitriding process results from: the constant oxide layer de-passivation and its chemical reduction on the surface, changes in the number of diffusion pathways and active centers to nitrides nucleation resulting from ion sputtering and shallow ion implantation. Moreover these effects are also associated with ability to increase of the gas phase activity due to ionization, which allows to influence on energy of nitrogen ions transported to the cathode and also to change the equilibrium of the process on the plasma-substrate interface [9]. Plasma nitriding is also characterized by same activity of the gaseous phase on the entire surface of the nitride element which provides homogeneous process conditions and satisfactory layer properties while during controlled gas nitriding process there are several difficulties which occur in a result of atmosphere flow inhomogeneity. The surface after ion sputtering is additionally chemically reactive that shortening the incubation stage for nitride phase nucleation. Therefore, such way of activation is also used before conventional chemical heat treatment processes [10]. Apart from the rapid heating of the surface, additional advantages of physical activation are also the dimensions reduction or cracking of the nitride elements at heating before saturation. However, ion activation has also some disadvantages associated with the excessive sputtering of the element edges called the edge effect, which makes the i.e. cutting edges blunt or causes the sputtering effect of the working surface of the element. Nevertheless, some solutions have already been found to prevent this type of effects, including pulse plasma nitriding and active screen plasma nitriding (ASPN) method on which authors will focus in this research and will compare its effects with conventional methods of nitriding.

2. Materials and methods

Nitriding processes were realized using Fe Armco with chemical composition presented in table 1. The microstructure of the material was ferrite with type III cementite (Fe_3C_{III}), grain size 9.5 μm, according to ASTM standard E1382-97.

TABLE 1

The chemical composition of Fe Armco

Material	**Element, % mass***										
Fe armco	C	Mn	Si	P	S	Cr	Ni	Mo	Cu	Al	Fe
	0.024	0.010	0.005	0.001	0.001	0.006	0.004	0.001	0.002	0.002	Rest
* SPECTRO ICP-MS spectrometer											

Mechanical surface activation of Fe Armco was realized using metallographic paper with grit from 220 to 2000. However, the ion activation of Fe Armco by cathode sputtering was realized during the heating the samples to the temperature of nitriding. The gas mixture used for cathodic sputtering was hydrogen and argon with 7:1 ratio. Controlled gas nitriding processes were realized with NITREX VVT nitriding furnace in cooperation with the industrial unit, according to the NITREG® technique. Nitriding processes were realized for the two stages: stage 1 – T = 763K, time = 1 h, atm. 100% NH_3, K_N = 20, stage 2 – T = 793K, time = 3 h, atm. 75% N_2/25% NH_3, K_N = 5,63. Cathode plasma nitriding (CPN) and the active screen plasma nitriding (ASPN) processes were realized in an JON-600 IMP nitriding furnace with a cooled anode using DORA POWER SYSTEM pulse power supplies, which provided the following parameters: T = 793 K, time = 3 h and 6 h, p = 150 Pa, atmosphere 75%H_2 – 25%N_2. Samples were placed directly on the cathode and also covered with an active screen. The cathode and the active screen elements were made of low carbon steel AISI 1010. The perforation of an active screen constituted of 80%. The distance between sample and active screen was 95 mm. To investigate the nitride layers after different techniques following tests were realized: microscopic observations using light microscopy (LM Carl Zeiss Axiovert microscope) and scanning electron microscopy – SEM (JEOL JSM-6610LV microscope). These methods have been used to evaluate the nitrided case depth, determine nitriding kinetics, examine the morphology, shape and dispersion of nitrides. Phase composition analysis was made using the X-ray GID and μ-XRD techniques (Empyrean PANalytical diffractometer). Additionally, for phase composition and diffusion effects analysis SEM-EBSD and SEM-WDS

methods (SU70 HITACHI microscope with Thermo Scientific analytical system) were used. Surface studies were realized with atomic force microscopy – AFM (AFM Veeco Instruments MultiMode microscope) in order to assess surface roughness and surface morphology after different nitriding processes.

3. Results and discussion

Literature review of nitriding subject indicates that in the past decade, due to the increasing quality requirements in automotive, aerospace, electro-engineering and biomedicine branches, innovative solutions have been also implemented in nitriding methods to shorten the process time, reduce over nitriding effects, (especially at the edges) and rapid changes in core and surface hardness or the nitrided layer flaking [11-13]. One of the solutions to eliminate mentioned problems is the active screen plasma nitriding method (ASPN). In this study, the effects of an active screen method on diffusive saturation of ferritic phase without alloying elements were investigated. The alloying elements might influence the nitrogen the nitrogen chemical activity. Thus the material without alloying elements was selected in order to avoid these changes. Additionally, conventional controlled gas nitriding process have also been realized in order to compare the structure of the Fe Armco surface layer and determine the advisability of applying a short time to this type of nitriding process (4 hours – 1 I stage + 3 II stage). It is known that the time of conventional controlled gas nitriding in industrial conditions ranges from few to several hours, and the generated diffusion layers are between few microns to even a few milimetres [14]. Furthermore authors based on their earlier research have determined that the use of plasma nitriding is favorable up to about 12 hours and considering active screen method, the applications of times of about 10 h for austenitic materials, and up to about 8 hours for ferritic materials is mentioned [15-18]. The microscopic tests presented in Fig. 1 have confirmed these thesis. Following phases after nitriding have been observed (analyse from the top): ε-$Fe_{2\text{-}3}N_{1\text{-}x}$ nitrides zone, with a nitrogen concentration from 4.55 to 11% mass. visible at 793K after controlled gas nitriding as a porous layer with characteristic centers of adhesion of the compound layer; the $\varepsilon + \gamma'$ zone consisting of a mixture of $Fe_{2\text{-}3}N_{1\text{-}x}$ and $Fe_4N_{1\text{-}x}$ nitrides which is formed from the ε zone decomposition during cooling visible as a homogeneous uniform layer both in the plasma nitriding processes (CPN and ASPN) and in controlled gas nitriding; the Fe_α(N,C) zone which constitutes of a nitrogen in ferrite solid solution in which nitrogen is located in the middle of the elementary cell with the parameters of: a_0 = 3.791÷3.801 Å.; the γ'-$Fe_4N_{1\text{-}x}$ nitrides zone, which precipitates from Fe_α(N,C) during cooling from process temperature to room temperature

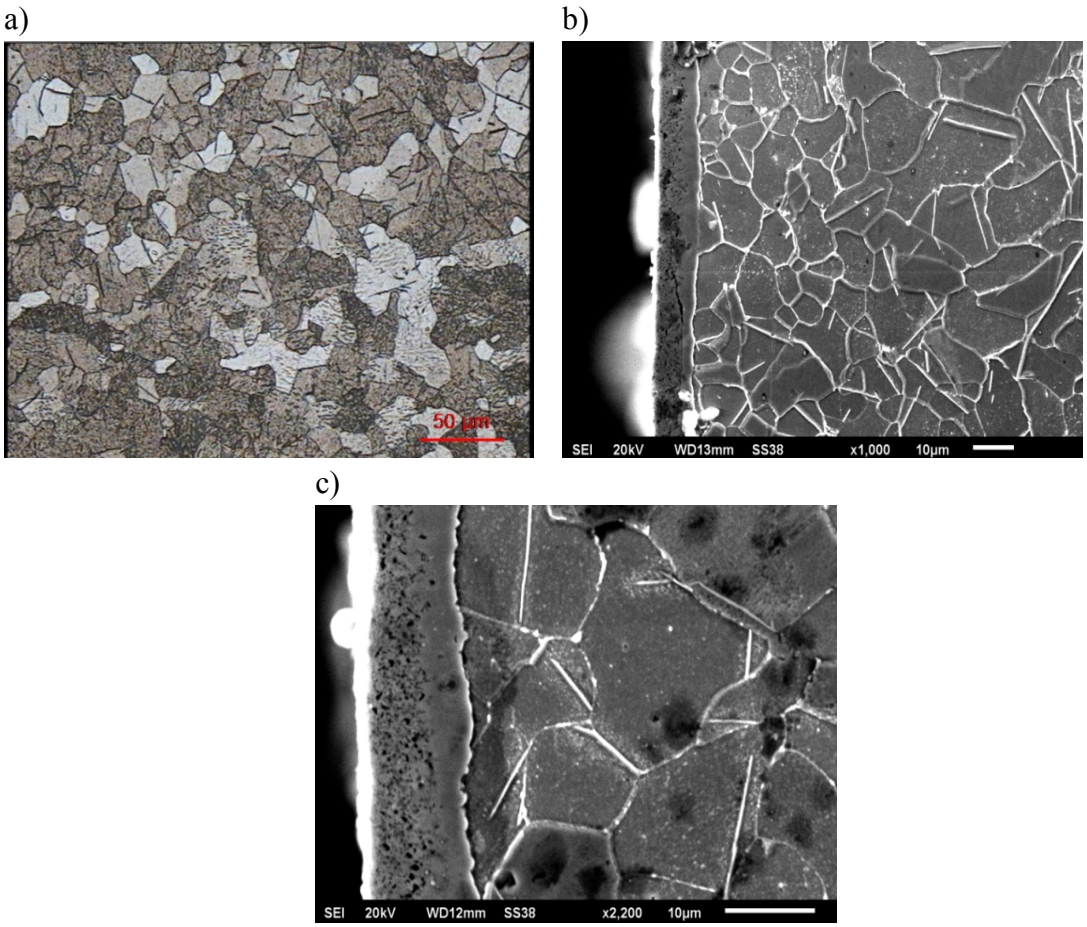

Fig. 1. Fe Armco microstructure after gas nitriding at 793K, nital etched; a) OM image of diffusion zone, process time 4 hours (1+3), b) SEM image of $\varepsilon/\varepsilon + \gamma'/\gamma'$ zone, process time 4 hours (1+3), c) SEM image of $\varepsilon/\varepsilon + \gamma'/\gamma'$ zone, process time 18 h (3+15)

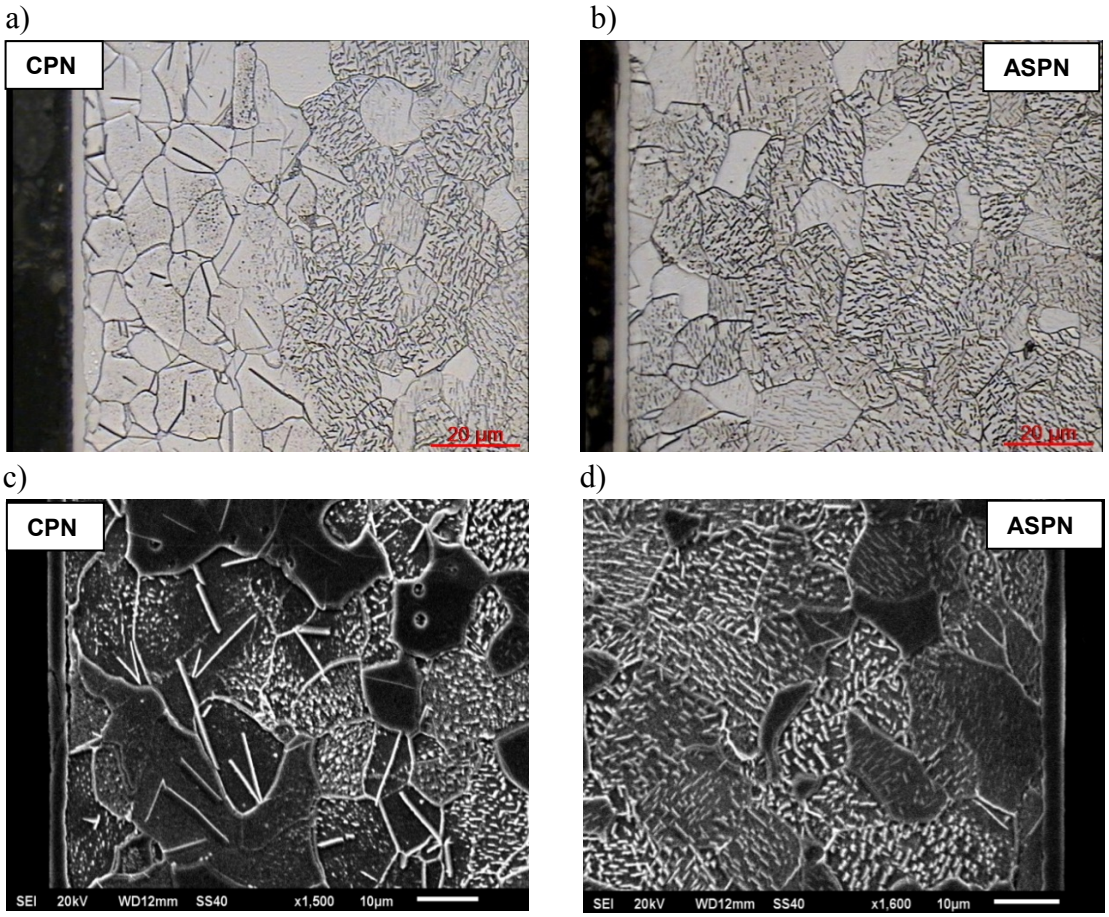

Fig. 2. Fe Armco microstructure after plasma nitriding – $\varepsilon/\varepsilon + \gamma'/\gamma'$ zone, 793K, time 3h, atm. 75%H_2 – 25% N_2, nital etched ; a) OM image after CPN process, b) OM image after ASPN process, c) SEM image after CPN process, d) SEM image after ASPN process

and have been observed as needle shaped coarse nitrides and fine dispersive nitrides depending on the nitriding process [19-22].

Fe Armco microstructures obtained after CPN and ASPN nitriding for 3 hours are presented in Figure 2.

Presented microstructures indicate that nitrided layer according to each process have various structures and thicknesses, which are in the range from 0.2 to 0.6 mm for plasma nitriding and from 0.3 to 0.85 mm for controlled gas nitriding process. This is related to variable phase growth rate at different stages of each process. According to the literature nitrided layer growth in each of the methods is affected by the temperature, time, pressure, nitrogen atmosphere activity, and in plasma nitriding the current-voltage parameters. The nitriding effects are also closely related to the mechanism of the slowest running processes at the surface and diffusion processes. Presented results show that for the nitriding temperature of 793K (520°C), the thickness of the nitrided layer change with the process time in a parabolic relation, which confirms that the slowest process is diffusion which is preceded by non-equilibrium surface processes resulting from the change of the balance of the thermodynamic processes such as: ionization, ion sputtering, implantation, deposition, chemisorption, nucleation, adsorption and re-deposition.

In order to explain the difference in crystallographic orientation of the nitrided layer phases SEM-EBSD tests were realized which allow to identify crystallographic orientation of the grains and confirm their effect on diffusion in different phases of the nitrided layer. Selected SEM-EBSD results are shown in Fig. 3. Based on the SEM-EBSD maps analysis it might be stated that there is a significant differentiation of the crystallographic planes orientation in the γ'+Fe_α(N,C) diffusion zone. A visible correlation with the emergence of (111) crystallographic orientation planes have been notice in Fe Armco after active screen plasma nitriding (ASPN). Consequently, nitrides nucleation occurs in grains with (001) orientation, which might result from the diffusion flux velocity change for this orientation and incomplete of the free spaces in octahedral voids, as compared to the (111) plane. This results in a varying nucleation effect and creates fine $\gamma'_{dispersion}$ – Fe_4N nitrides and is a confirmation of the previously described assumptions concerning nitrides nucleation in nitrogen saturated ferrite. Changing the nitrogen diffusion flux in the (001)-oriented grains will change the nitrogen concentration on the surface, enhance nitrides decomposition and generate equilibrium precipitates. Nitrogen diffusivity depends mainly from the crystallographic orientation and it has been presented that this process diverse and is greater for (101) and (001) planes than for (111) planes. A significant change in crystallographic planes orientation is also visible from the SEM-EBSD maps analysis from the $\varepsilon + \gamma'$ solution zone. The arrangement of the planes highlights the mechanism of the growth of the discussed zone and confirms its significant contribution in the formation

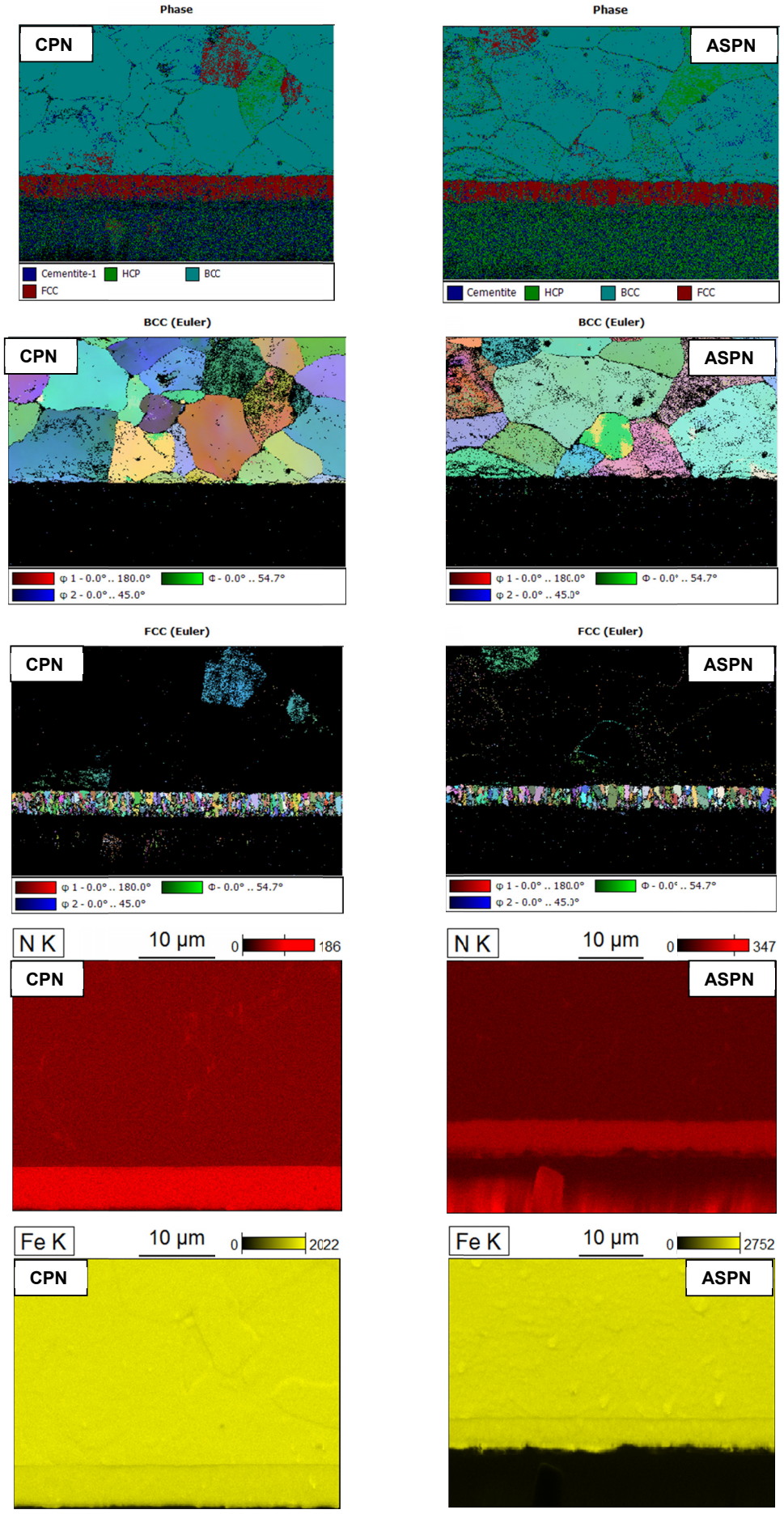

Fig. 3. SEM-EBSD and Euler's maps of Fe Armco after CPN and ASPN, 793K, 6h

of the diffusion zone. Depending on the crystallographic plane orientation at the $\varepsilon + \gamma'/\gamma' + Fe_\alpha(C,N)$ interface, it may be stated that nitrogen diffuse into the diffusion zone by diffusion pathways, which constitute from the incompletely settled gaps in the (101) and (001) crystallographic planes (Fig. 3). Nitrogen atoms are transferred to the nucleation areas of the γ' nitrides as a result of the change of nitrogen concentration at the $\varepsilon + \gamma'/\gamma' + Fe_\alpha(C,N)$ interface. Additionally the diffusion flux intensity depends from the number of active centers, including grain boundaries of the preferably oriented crystallographic planes.

X-ray diffraction tests have confirmed that the differences between CPN and ASPN is a consequence of the surface layer defects, which is also resulted from the metastability of Fe-N compounds and rebuilding their crystal structure, after nitriding. The Fe Armco GID diffractogram shows only the strongest reflections recorded for angles $2\theta = 45°$ and 65°, which confirms the presence on the surface the Fe_α phase with (110) and (200) crystallographic orientation. The XRD-GID analysis indicates after the nitriding at 793K for 3 and 6h in both CPN and ASPN methods, $\varepsilon - Fe_{2\text{-}3}N + \gamma' - Fe_4N$ phase with crystallographic orientation $(111)_\gamma // (002)_\varepsilon$ (reflection corresponding to the angle $2\theta = 41.5°$) registered for both phases (Fig. 4).

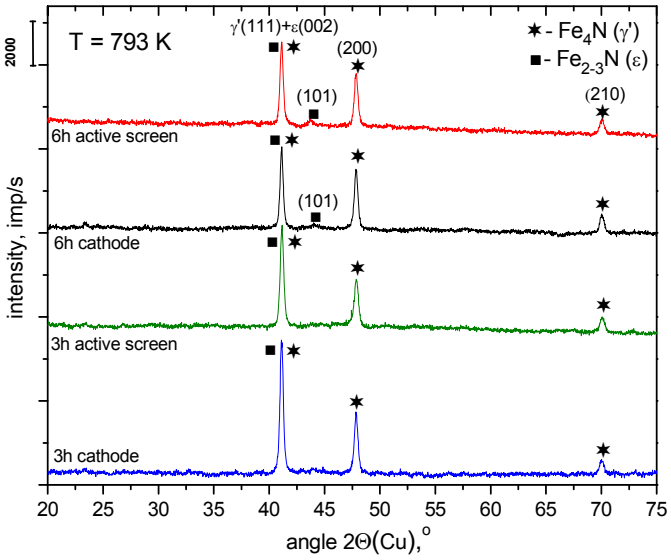

Fig. 4. XRD-GID diffractogram of Fe Armco after CPN and ASPN at temperature 793K

Intensive peak from the γ'-Fe_4N phase is also visible at $2\theta = 47.5°$ which correspond to the crystallographic orientation (200). In ASPN method this indicates the effect of much slower saturation and leads to the reduction of its thickness or the absence of the process at a low temperature (due to a complete passage to the γ'-Fe_4N phase). However, low intensity reflections occur for the $\varepsilon - Fe_{2\text{-}3}N$ phase in the range of the angle $2\theta = 44°$ in the processes lasting for 6h. This is due to the increase in the $\varepsilon + \gamma'$ solution zone with simultaneous duration and nitriding temperature growth. This is confirmed by the microstructure analysis, the structure and its assumed growth mechanism. It can also be noted that for a short duration of the nitriding process, i.e. 3, 6 h, the nitriding intensity in the case of ion methods is comparable to conventional gas nitriding and the growth kinetics of the nitrided layer in the ion methods applied differ slightly (see Fig. 5).

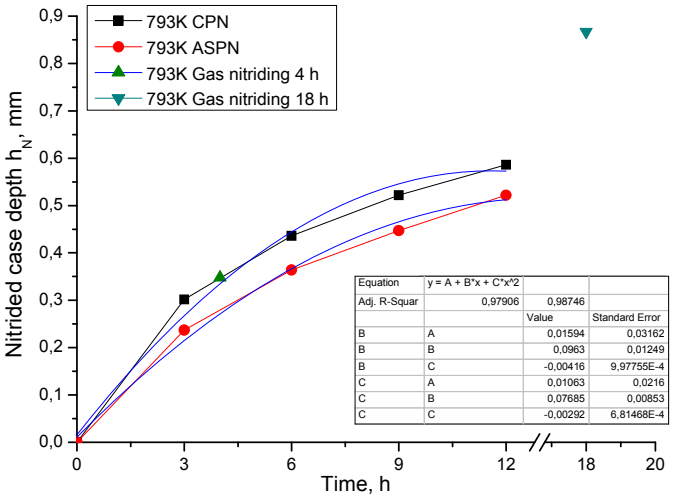

Fig. 5. The nitrided layer thickness change h_N, for applied methods and times of nitriding at 793K

The results of the nitrided layer growth calculations show that with the lengthening process duration, differences disappear in surface layer saturation speed. Thus, it can be concluded that the application of ion nitriding process is beneficial up to about 9 h, which concurs with the results obtained by Lachtin et al. [23] on plasma nitriding as well as with the results obtained in the active screen methods [24,25]. The inspiration for choosing a short nitriding time was the analysis of the depth of γ'-$Fe_4N_{1\text{-}x}$ nitride zones, both coarse and dispersive. As reported in the literature, increasing share of needle shaped Fe_4N nitrides in the nitrided layer of ferritic steels, due to their shape and arrangement, increases the brittleness of the generated layer and its tendency to flake due to external mechanical stresses. In addition, it changes the stress state compared to the ductile ferrite core [26,27]. This indicates change of the nitrogen concentration profile in the surface layer in the presence of active screens. However, it is characteristic for this method that for each applied time, the share of $\gamma'_{dispersive}$ nitrides is larger compared to the effects after CPN and much larger (about 3 times) as compared to conventional gas nitriding, as demonstrated in Figure 5. This indicates that in the presence of active screens (AS), in the course of ion nitriding, a change in the nitrogen distribution profile in individual zones appears. Another reason for choosing a short nitriding time was to obtain a nearly constant thickness of the γ'_{coarse} zone, though different for the CPN and ASPN methods (approx. 3 times) but much smaller compared to the effects of gas nitriding. As far as the thickness of the $\gamma'_{dispersive}$ zones is concerned, in the case of the ion nitriding time applied, a growth of this area is observed, which occurs most intensely up to the time of 6 hours, opposed to gas nitriding method. After a longer nitriding time it might be observed the tendency to reduce the thickness of the zone and a final levelling for approximately 12 hours (or

longer). However, attention should also be paid to the differences in the first, $\varepsilon/\varepsilon + \gamma'$, zone. In the case of a layer obtained by gas nitriding process, the presence of a $\varepsilon/\varepsilon + \gamma'$ zone of 9 to 17 microns' thick, namely twice higher as the total thickness of the nitrided layer, compared to ion nitriding process. However, in both variants of ion nitriding, the $\varepsilon/\varepsilon + \gamma'$ zone is smaller and ranges from approx. 2.5 to 6 µm. The growth of this zone is hyperbolic, which is associated with the chemical reactions at the atmosphere – substrate interface, its catalytic interaction with the gas phase at the interface, changing the nitriding atmosphere potential in the case of conventional gas nitriding, conditions of the active nitriding atmosphere ionization and its composition in the case of ion nitriding. Surface topography after nitriding varied significantly and depends largely on its parameters. One should keep in mind that the analyzed surface is a mixture of $\varepsilon/\varepsilon + \gamma'$ phases in the surface zone of the nitrided layer obtained for a given process after various effects of nitrogen saturation. The results obtained by the AFM method show that in ASPN processes, compared to CPN ones, a significant change in the surface morphology and roughness parameter has been observed. Surface topography parameters of the nitrided layer presents the biggest differences. In the case of AFM, measurements were carried out in the area of 5×5 µm, and the resulting 3D image clearly reveals a polished Fe Armco surface after the grinding process. The roughness parameter values in this case are in the range of R_a from –72.8 to 88.5 nm (Fig. 6).

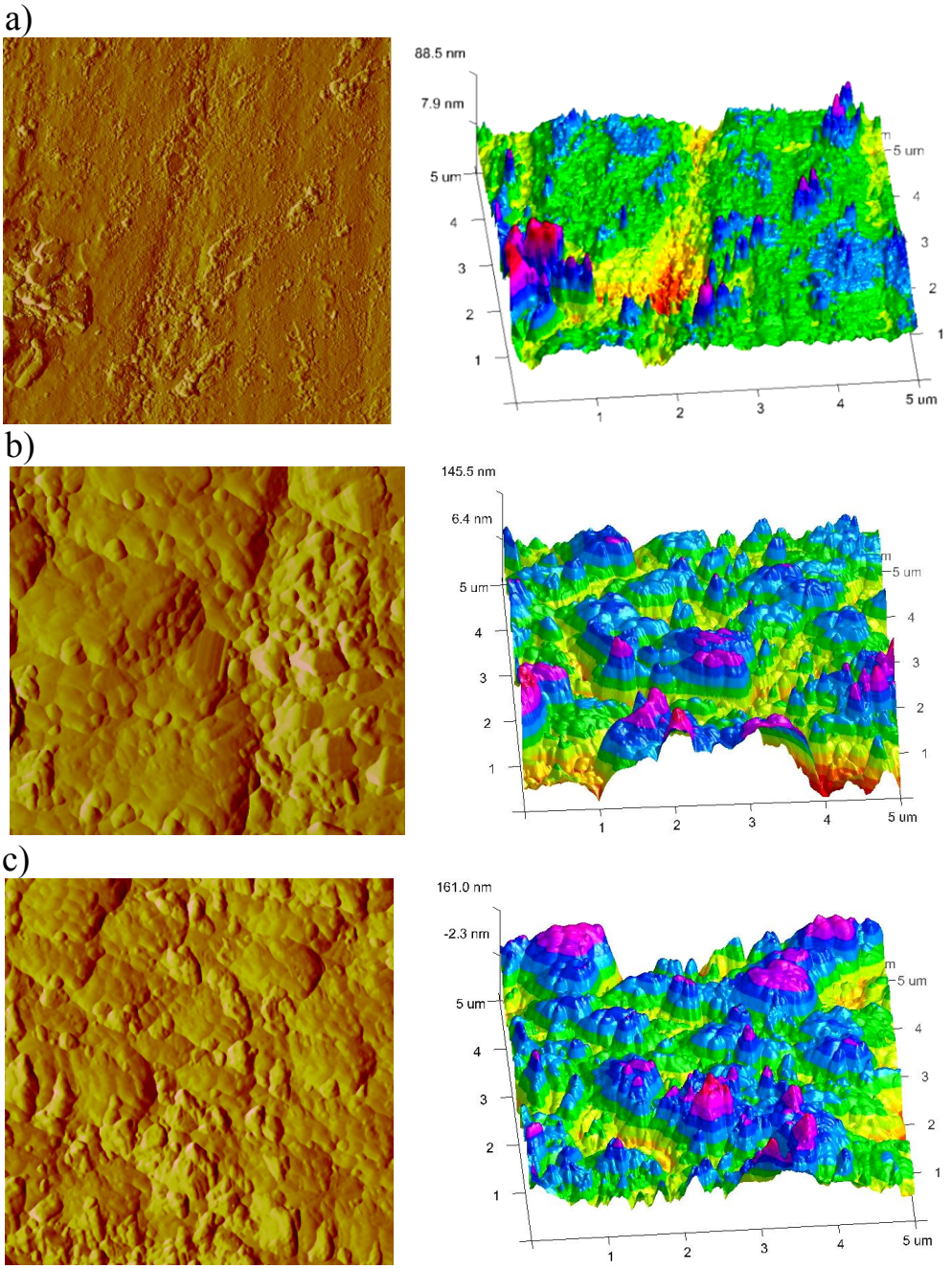

Fig. 6. The (AFM) Fe Armco surface topography, scan area 5×5 µm a) before nitriding processes – 2D / 3D image, b) after ASPN ion nitriding (793K, 6h) – 2D / 3D image, c) after CPN (793K, 6h) – 2D / 3D image

For the ion nitriding parameters herein discussed, the roughness parameter R_a equals to 0.04 μm, both in CPN and in ASPN. However, the 2D and 3D surface images point to significant differences in its topography. A lower roughness parameter in the range of R_a from –93.8 to +91.3 nm was observed on the surface after ASPN process for 3 hours. This is confirmed by the 3D map, where characteristic small globules with a polished surface can be found. This is probably a consequence of the effect associated with bombarding the surface with high-energy ions/particles and the surface growth of the nitride phases mixture during slow cooling after nitriding. On the other hand, taking into account the surface after ion nitriding at 793K for 6h it can be observed that it also has a lower roughness parameter R_a for ASPN, compared to CPN. The surface roughness parameter in the range of R_a from –132.8 to +145.5 nm in ASPN, and R_a from –165 to +161 nm in CPN, are presented in Figure 6b,c. The globular surfaces visible on the 3D map indicate the effects of higher surface polishing after the active screen method. It is known that the phenomena occurring at the surface leads to the reduction in its energy states, thus it can be assumed that after the active screen nitriding, surface energy differs compared to CPN. Given that the visible nitriding effects are a direct surface condition before completing the saturation surface layer process, related also to the applied cooling conditions, it can be concluded that the surface formed by using the active screen method is favorable in the light of reducing residual stresses occurring in the $\varepsilon + \gamma'$ or $\varepsilon/\varepsilon + \gamma'$ zones and directly under the layer, resulting from surface strengthening during mechanic activation. Having analyzed ion nitriding processes at 793K, a significant effect of the active screens' impact can be noticed. This effect is associated to the lack of the γ'_{coarse} nitrides, even in a 6-hour-process, which in turn leads to obtaining nitrided layers with high homogeneity and uniformity. One of the hypotheses concerning the absence of γ'_{coarse} nitrides in ASPN is a reduced intensity of cooling due to the use of the active screen, which affects slowing down the $\gamma'_{dispersive}$ nitrides re-fragmentation processes as a result of the tendency of the nitride precipitates system to reduce energy. In the case of ASPN, this effect is of utmost technological importance. During the chemical heat treatment at a given temperature, saturation velocity depends on surface processes and diffusion. It is the slowest ones which decide on process kinetics. In the case of the ion nitriding processes, it should be assumed that the impact of the phenomena mentioned occurs for specific zones of the nitrided layer. In the zonal structure of the investigated Fe Armco, the effects of the impact of these phenomena should be divided into the surface zone, diffusion zones and the nitrided material matrix.

4. Conclusions

The encouraging results in solving the problems of ion nitriding with the ASPN method, obtained by the Authors, may give rise to a further development of active screens (AS) applications in the field of surface engineering and chemical heat treatment. The presented method is not only attractive due to the economic aspects associated with low energy processes, but also the ecological aspects, such as a significant reduction in the emission of harmful gases and chemical solutions for materials surface cleaning and degreasing. The application of active screens (AS) is favorable for short nitriding times 3, 6 hours and the temperature of 793K, whereas for longer times and a higher temperature there is a difference of up to about 10% in the thickness and hardness of the nitrided layers. The effects of ion nitriding are determined not only by the presence of an active screen, but also by the physical Fe Armco surface activation during ion sputtering, strengthening and defecting the surface layer in the process of mechanical activation at the stage of Fe Armco preparation to nitriding. Phenomenon of recrystallization, conducive to increasing the concentrations of nitrogen in the strengthened zone, resulting from the fragmentation of the structure and an increase in grain boundaries share in the diffusion active centers is of crucial importance. The attractiveness of ASPN process is also associated with the change in the morphology of γ'-Fe_4N nitrides precipitates in the diffusion zone nitrided with Fe Armco. As a consequence the active screens on the surface and diffusion leads to obtaining diffusive zones without adverse balanced partial divisions of needle-shaped γ'-Fe_4N nitrides precipitates and reduction of the $\varepsilon + \gamma'$ solution zone. The ASPN method is particularly useful, not only in terms of the low energy consumption in the process, but also due to the reduction in the temperature of the process and changing the driving force of the nucleation phase during nitriding at <793K and nucleation nano-effects in the material. Finally this allows a wide variety of process parameters to optimize the technology and modelling the mechanism and morphology of the nitrided layers.

REFERENCES

[1] T. Burakowski, T. Wierzchon, Surface Engineering of Metals, 1995 WNT Editors, Warsaw.

[2] J. Michalski, J. Iwanow, J. Tacikowski, I. Sułkowski, P. Wach, T.N. Tarfa, J. Tymowski, Anti-corrosion nitriding, with post-oxidation and inhibitor impregnation, and its industrial applications, H. Treat. Met. **31**, 31-35 (2004).

[3] J. Tacikowski, J. Zysk, Controlled gas nitriding NITREG, Metal Science and Heat Treatment **63**, 26-29 (1983) (in polish).

[4] J. Zysk (Ed.), The iron alloys gas nitriding development, 2008 IMP Editors, Warsaw (in polish).

[5] D.K. Inia, A.M. Vredenberg, F.H.P.M. Habraken, D.O. Boerma, Nitrogen uptake and rate limiting step in low-temperature nitriding of iron, J. Appl. Phys. **86**, 810-816 (1999).

[6] T. Czerwiec, H. Michel, E. Bergmann, Low-pressure, high-density plasma nitriding: mechanisms, technology and results, Surf. Coat. Tech. **109**, 182-190 (1998).

[7] K.J.B. Ribeiro, R.R.M. De Sousa, F.O. De Araujo, R.A. De Brito, J.C.P. Barbosa, C. Alves Jr., Industrial application of AISI 4340 steels treated in cathodic cage plasma nitriding technique, Mat. Sci. Eng. A **479**, 142-147 (2008).

[8] T. Wierzchon, I. Ulbin-Pokorska, K. Sikorski, J. Trojanowski, Properties of multicomponent surface layers produced on steels by modified plasma nitriding processes, Vac. 53, 473-479 (1999).

[9] D. Moszynski, I. Moszynska, W. Arabczyk, Iron nitriding and reduction of iron nitrides in nanocrystalline Fe-N system, Mat. Lett. **78**, 32-34 (2012).

[10] J. Baranowska, K. Szczecinski, M. Wysiecki, Growth of nitride layer after cathode sputtering, Vac. **70**, 293-297 (2003).

[11] C.A. Figueroa, F.T. Alvarez, New pathways in plasma nitriding of metal alloys, Surf. Coat. Tech. **200**, 498-501 (2005).

[12] S. Corujeira Gallo, H. Dong, New insights into the mechanism of low-temperature active-screen plasma nitriding of austenitic stainless steel, Scri. Mater. **67**, 89-91 (2012).

[13] X.L. Wu, W. Zhong, N.J. Tang, H.Y. Jiang, W. Liu, Y.W. Du, Magnetic properties and thermal stability of nanocrystalline ε-Fe_3N prepared by gas reduction-nitriding method, J. Alloys Compd. **385**, 294-297 (2004).

[14] S.A. Gerasimov, V.A. Golikov, M.A. Gress, G.G. Mukhin, V.I. Snop, High-pressure gas nitriding of steels, Met. Sci. Heat Treat. **46**, 227-229 (2004).

[15] T. Fraczek, M. Olejnik, J.J. Jasinski, Unconventional short-term glow discharge nitriding of 316L austenitic steel, Mat. Sci. Forum **654-656**, 366-369 (2010).

[16] X. Xiaolei, W. Liang, Y. Zhiwei, H. Zukun, A comparative study on microstructure of the plasma nitrided layers on austenitic stainless steel and pure Fe, Surf. Coat. Tech. **192**, 220-224 (2005).

[17] S.C. Gallo, H.H. Dong, Study of active screen plasma processing conditions for carburising and nitriding austenitic stainless steel, Surf. Coat. Tech. **203**, 3669-3675 (2009).

[18] A. Nishimoto, K. Nagatsuka, R. Narita, H. Nii, K. Akamatsu, Effect of the distance between screen and sample on active screen plasma nitriding properties, Surf. Coat. Tech. **205**, 365-368 (2010).

[19] M. Kulka, P. Dziarski, N. Makuch, A. Piasecki, A. Miklaszewski, Microstructure and properties of laser-borided Inconel 600-alloy, Appl. Surf. Sci. **284**, 757-771 (2013).

[20] P. Hubbard, J.G. Partridge, E.D. Doyle, G.D. McCulloch, M.B. Taylor, S.J. Dowey, Investigation of nitrogen mass transfer within an industrial plasma nitriding system I: The role of surface deposits, Surf. Coat. Tech. **204**, 1145-1150 (2010).

[21] A. Sokolowska, J. Rudnicki, P. Beer, L. Maldzinski, J. Tacikowski, J. Baszkiewicz, Nitrogen transport mechanisms in low temperature ion nitriding, Surf. Coat. Tech. **142-144**, 1040-1045 (2001).

[22] Y.D. Kogan, V.E. Kol'tsov, Effect of plasma nitriding on mechanical properties of refractory metals and alloys: nitriding in engineering, Transactions MADI **174**, 135-145 (1979).

[23] Y.M. Lakhtin, Y.D. Kogan, Gas nitriding of engineering components and tools, Mashinostroenie Moscow, 60 (1982).

[24] T. Fraczek, M. Olejnik, J.J. Jasiński, Z. Skuza, Short-term low-temperature glow discharge nitriding of 316L austenitic steel, Metal. **50**, 151-154 (2011).

[25] H.J. Spies, H.L. Thien, H. Biermann, Verhalten von Staehlen beim Plasmanitrieren mit einem Aktivgitter (Behaviour of steels in active screen plasma nitriding), HTM Z Werkst. Warme. Fertig. **60**, 1-8 (2005).

[27] L. Lefevre, T. Belmonte, T. Czerwiec, A. Ricard, H. Michel, Measurements of nitrogen atom loss probability versus temperature on iron surfaces, Surf. Coat. Tech. **116-119**, 1244-1248 (1999).

[28] D. Nolan, V. Leskovsek, M. Jenko, Estimation of fracture toughness of nitride compound layers on tool steel by application of the Vickers indentation method Surf. Coat. Tech. **201**, 182-188 (2006).